ENHANCING GRAPHITIC CARBON CONTENT OF CARBON-BASED ELECTRODE MATERIALS BY PULSED ELECTROPHORETIC DEPOSITION FOR ELECTROCHEMICAL CAPACITOR

K.T. Lau[1], M.A. Azam[2], M.E.A. Manaf[2], M. Zaimi[2], M.S.M. Suan[2], N.A. Yaacob[2], J. Narayanasamy[3] and K.F. Samat[4]

[1]Advanced Manufacturing Centre, Fakulti Teknologi Kejuruteraan Mekanikal dan Pembuatan, Universiti Teknikal Malaysia Melaka, Hang Tuah Jaya, 76100 Durian Tunggal, Melaka, Malaysia.

[2]Advanced Manufacturing Centre, Fakulti Kejuruteraan Pembuatan, Universiti Teknikal Malaysia Melaka, Hang Tuah Jaya, 76100 Durian Tunggal, Melaka, Malaysia.

[3]Infineon Technologies (Malaysia) Sdn. Bhd., Melaka, Malaysia.

[4]Department of Mechanical Systems Engineering, Graduate School of Engineering, Tohoku University, 6-6-01 Aramaki-Aza-Aoba, Aoba-ku Sendai 980-8579, Japan.

Corresponding Author's Email: [1]ktlau@utem.edu.my

Article History: Received 12 January 2018; Revised 6 June 2018; Accepted 17 September 2018

ABSTRACT: Crystallinity of carbon electrode materials and their deposition techniques are the crucial factors for electrochemical capacitor (EC) performance. The present work investigates deposit yield and graphitic content of activated carbon (AC) and CNT coatings deposited by pulsed electrophoretic deposition (EPD). Pulse voltage with pulse separation times of 30 to 50 s, alternated with the long pulse width (i.e. 2.5 min) was applied. Although the pulse separation time at 30 s reduced the CNT coating yield, its graphitic content increased by 40 % as compared to the CNT coating deposited by continuous voltage EPD, as indicated by the I_G/I_D ratio of Raman spectra. However, graphitic content increase was not observed in the deposition of AC. Consequently, the CNT deposition gained a higher graphitic-nongraphitic content ratio than the AC. This finding opened up the possibility of the EC performance enhancement by the graphitic CNT control in electrode materials through EPD process.

KEYWORDS: *Specific Capacitance; Carbon Nanotube; Activated Carbon; Crystallinity; Electrophoretic Deposition*

1.0 INTRODUCTION

Carbon nanotube (CNT) and activated carbon (AC) electrochemical capacitors (EC) is advantageous for applications that require fast response and long energy retention [1]. Current dominant energy storage devices such as high-energy density lithium ion battery is larger in size than the supercapacitor for the same power capacity. Nevertheless, the former has low power density and poor energy retention [2].

EC set up composes active electrode materials deposited on metallic collectors in the EC. The electrode materials are the predominant factor on the EC's energy density performance, in addition to deposition techniques and electrolytes [2-3]. As for now, carbon materials such as graphite, graphene, AC and CNT are still the dominant EC's active electrode materials [4]. These carbon materials have good electrical, mechanical, chemical and thermal properties. Furthermore, they have very large specific surface area which help to increase the specific electrochemical energy storage capacity of EC [3-5].

The active electrode materials made of carbon materials require high temperature and harsh chemicals to produce. However, the synthesis process and materials properties of the carbon materials as active electrode materials for supercapacitors have been established [4]. A recent study reported metal–organic frameworks (MOFs) materials, which are extremely porous, sponge-like structures as a potential candidate for EC's electrode materials [1]. However, the MOFs are not very electrically conductive, thus require further investigation as a potential replacement of carbon electrode materials [1].

Electrophoretic deposition (EPD) has been used for the carbon electrode material deposition because of its simple set-up and control flexibility [3, 6-7], serving as an alternative deposition technique for chemical vapour deposition (CVD) [8-9] and arc discharge [10]. Previous studies show that EPD in pulsed mode improves the deposit density and enhances particle alignment of CNTs [3,9]. Since deposition in pulsed mode at increasing pulse frequency (i.e. at high frequency range) reduced the deposit yield [6, 11-13], the yield gain can be improved by the increase of pulse width (i.e. refer as voltage

ON time) and applied voltage [11, 14-16]. In one pulsed voltage cycle, one pulse width is followed by one pulse separation time (i.e. voltage OFF time). The pulse separation time is the time when the applied voltage is switched off. During the switching of voltage from ON to OFF mode (particularly for high voltage), inertia forces is the predominant driving force for particle movement toward the depositing substrate. Under this scenario, particles in the EPD suspension are accelerated and only slowed down after some time [11]. A longer pulse separation time may provide time for the moving particles to adjust from turbulent into the streamline flow, which is good for the uniform deposition [6]. Furthermore, the streamline flow reduces Joule heating effect created by the high applied voltage [11].

This paper reports the deposit yield and graphitic content results of pulsed EPD of AC and CNT coatings obtained at different pulse separation times and applied voltages. Possible deposition mechanism of the pulsed EPD of both carbon-based electrode materials is presented. To the best of our knowledge, there is no study reported on the pulsed EPD involving pulse EPD time (total time of pulse width and pulse separation time) more than one minute, particularly in the deposition of carbon electrode materials for electrochemical capacitor.

2.0 EXPERIMENTAL DETAILS

Particle suspensions of 0.4 mg/mL AC (batch AC) were prepared by mechanical mixing of AC particles (Kuraray, RP20, specific surface area of 1800 m^2/g) in a pure isopropanol medium. A similar suspension preparation process was used to prepare batch CNT using CNT particles (Sigma-Aldrich, 412988, multi-walled, 7-15 nm × 0.5-10 μm, SSA 2200 m^2/g). In both batches, $Mg(NO_3)_2$ charging additive and polyvinylpyrrolidone (PVP) binder were added at 10 wt% from the suspension particles basis. Then, the mixture underwent ultrasonication for 20 minutes in ambient environment to achieve homogeneous dispersion.

Ni-Fe alloy sheet (YEF50-grade, Hitachi Metals Ltd) with a thickness of 0.2 mm was used as the metallic support for the carbon active materials of the EC. The sheet was cut into 15 mm diameter circular substrates and then rinsed with distilled water. Subsequently, the substrate was fixed as cathode, parallel to the graphite rod counter electrode (diameter = 6 mm, Gamry Instruments) at 20 mm separation. Both were connected to DC power supply (model:

EC1000XL, Fisher Scientific) and immersed into suspension. Prior to EPD process, the suspension underwent 60 min magnetic stirring. AC and CNT coatings were deposited at DC voltages of 20, 50 and 80 V for different pulse separation times (i.e. 30, 40 and 50 s). For each EPD sample, four voltage pulses with total deposition time (inclusive of ramp-up time) of 10 min were applied. Pulse separation time between the voltage pulses was fixed at 30, 40 or 50 s. Illustration of the pulsed voltage versus time profile is shown in Figure 1. Controlled AC and CNT coating samples were prepared by EPD process at constant 80 V for continuous deposition time of 10 min (i.e. pulse separation time = 0 s).

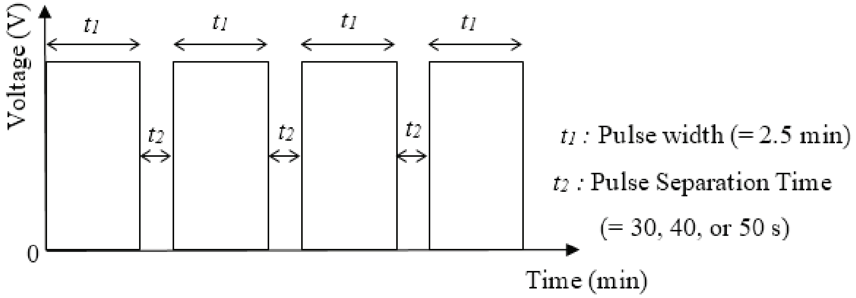

Figure 1: Pulsed EPD process's pulsed voltage–time profile

The coating yields of pulsed EPD samples were determined by subtracting the deposited Ni-Fe sheet's weight with the blank Ni-Fe sheet. Sample weighing was conducted by a high precision weighing balance (0.01 miligram resolution, Mettler Toledo) after the samples were air dried at 120°C for 2 hr. Their surface microstructures were captured using scanning electron microscopy (scanning electron mode, accelerating voltage = 15 kV, Carl Zeis AG, Model: Evo 50). The extent of graphitic carbon content in the coatings was measured by Raman spectroscopy (solid-state laser, 4 mW laser power, laser beam wavelength = 532 nm, laser spot size = 1 μm, exposure time = 1 s, model: uniRAM-3500).

3.0 RESULTS AND DISCUSSION

Deposit yield of the AC samples by pulsed EPD increased with the increase of applied voltage for three different pulse separation times (see Figure 2). The deposition at pulse separation times of 40 s and 50 s shows a linear increase of deposit yield versus applied voltage, which is consistent with Hamaker's law [17]. For the 30 s sample, the deposition at 80 V only recorded a slightly higher yield than at 50 V, thus it exhibited a nonlinear trend. Since the EPD yield was directly corresponding to the suspension particle conditions prior to the EPD, AC particle deposition behaviour were explained in terms of the DLVO theory (named after Derjaguin, Landau, Verwey and Overbeek) and electric double layer (EDL) compression mechanism [12,18].

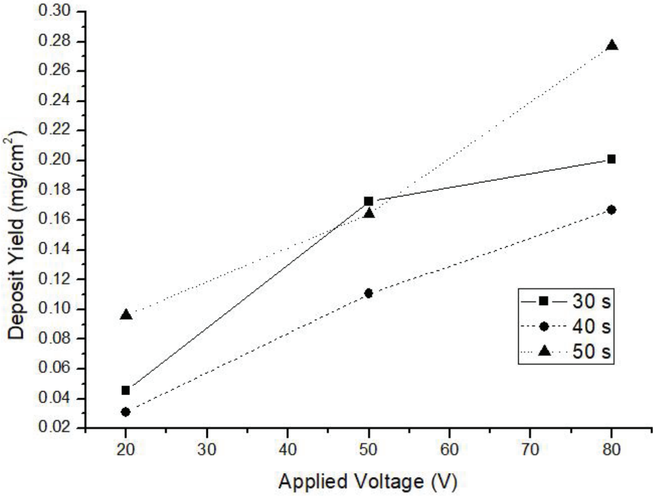

Figure 2: Deposit yield of AC coatings deposited at different pulse separation times as function of applied voltage

A longer pulse separation time indicates longer suspension time for AC particles without applied electric field and mechanical agitation. For instance, at pulse separation times of 40 and 50 s, AC particles were suspended without the external forces for total additional 30 and 60 s respectively when compared to AC particles deposited at pulse separation of 30 s. The DLVO theory indicates that the suspension particles are surrounded with EDL and the mutual repulsive EDL maintains the particles in a stable dispersion. As the applied voltage was turned on (during the voltage ON time), the interaction between the EDL and applied electric field resulted in the distortion and compression of the particles' EDL when moved toward the oppositely charged cathode. This weakened the repulsive electrostatic forces of the CNT particles formed by the particles' EDL [12,18], resulted in the dominancy of attractive Van der Waals forces, causing the particles to agglomerate [12,18].

As the total suspension time (= pulse width + pulse separation time), the percentage of the AC agglomerates increased and more of them were deposited. However, their inherent weak interparticle bonding resulted in a significant deposit yield loss through disintegration during EPD process. Figure 2 shows a lower yield was obtained by the 40 s sample as compared to the 30 s sample. It is presumed larger amount of agglomerates were deposited on the 40 s samples due to longer total suspension time. The deposit loss caused by deposited agglomerates was also observed in the 30 s sample when the applied voltage increased from 50 to 80 V. This may be caused by a higher collision rate of the incoming particles at a high applied voltage.

The 50 s sample of AC produced higher yields than the 30 and 40 s samples. It is suggested that the amount of agglomerates in the corresponding EPD suspension reduced significantly with the prolonged EPD time, due to the ongoing agglomerate sedimentation. Thus, fewer agglomerates were supposedly deposited on the 50 s sample due to longer total suspension time. The lower percentage of deposited agglomerates may contribute to a higher coating bonding strength and lower coating loss (i.e. higher yield) [12].

Contradictory to the AC samples, the CNT samples exhibited three different deposit yield trends (see Figure 3). The 30 s sample shows a linear yield increase in the studied voltage range. This is consistent with the Hamaker's law [17]. Whereas, the 40 s sample shows a nonlinear yield curve, in which yield increase at 20-50 V range but reduced at 50-80 V range. However, the 50 s sample maintained a constant yield from 20 to 50 V at ~0.11 mg/cm^3 (higher than the 30 s and 40 s samples). A subsequent yields drop at 50-80 V range of the 50 s samples may be caused by a higher collision rate of the incoming particles at a high applied voltage.

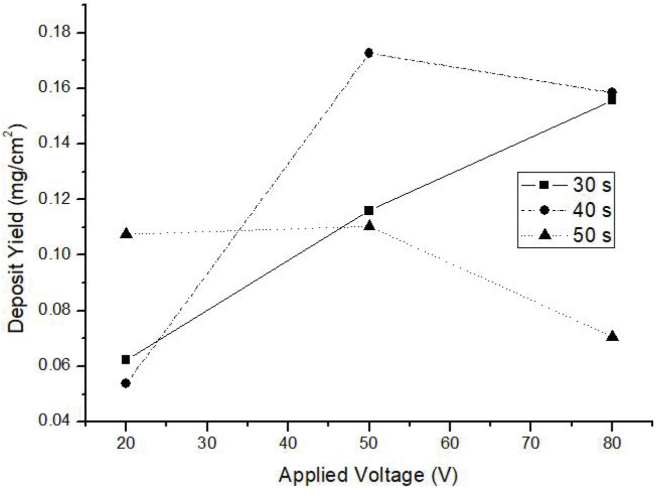

Figure 3: Deposit yield of CNT coatings deposited at different pulse separation times as function of applied voltage

The CNT and AC samples are presumed to behave similarly in terms of their surface charge formation and the interaction with the suspension medium because of similarity in the formulation and carbon element. Thus, the CNT yield trend was also explained using the same deposition mechanism that was applied to the AC deposition. Nevertheless, the CNT particles are anisotropic and have smaller weight than the isotropic AC particles [19-20]. Figure 4 shows that the EPD-deposited CNT particles have a larger surface area (7-15 nm diameter × 0.5-10 μm length) compared to the EPD-deposited AC particles (particles size up to 10 μm). It is likely that the CNT particles have higher tendency than the AC particles to agglomerate in the suspension prior to the EPD, because of its higher surface area. Moreover, the agglomerated CNT particles are comparatively lighter in weight than the agglomerated AC particles because of smaller individual particles size and weight. Thus, the CNT agglomerates tend to be more stable than the AC agglomerates and may participate in the EPD process. As the applied voltage increased, more CNT particles agglomerates were deposited at a faster rate, creating more disorganized CNT coating [12]. Because of a longer pulse separation time might create more agglomerates suspension and subsequently deposited agglomerates, the corresponding interparticle bonding in CNT coating became weaker, created a higher yield loss in the CNT samples at the high pulse separation time. Instead of observing yield gain with the increasing voltage, the CNT's yield dropped at high voltages (i.e. 50 and 80 V) for the high pulse separation time samples (i.e. 40 and 50 s). As a result, pulsed EPD using CNT particles obtained lower yields than the AC particles at the same EPD parameters.

Graphitic contents of AC and CNT coatings prepared at different pulse separation times were investigated using Raman spectra (see Figure 5). It is believed that the AC and CNT with the graphitic (viz. honey-comb) crystal structure is capable to conduct more efficiently the electricity in the EC's electrode materials than the non-graphitic structure [21]. The Raman results show the D- and G-band peaks intensities of the current AC and CNT coatings varied with the increasing pulse separation time. D-band peak intensity is equivalent to the carbon defects content associated with vacancies and carbonaceous impurities that destroy the graphitic symmetry of the CNT crystal structure (which is represented by the G-band peak) [21-22]. D- and G-band peaks intensities of the AC coating increased at a longer pulse separation time. Similarly, the CNT coatings also show increasing band peaks intensities trend at longer pulse separation times. Raman peak intensity of the AC and CNT deposits were controlled by laser scattering at analyzed spot area. Since AC or CNT deposits formed using different pulse separation times have completely different surface microstructures (see Figures 4), the cause of the increasing peak intensity with the increase of the pulse separation time could not be established. Consequently, ratio of their G- over D-band peaks (i.e. I_G/I_D) was used to compare the extent of structural defects in the graphitic structures of the deposits (i.e. caused the presence of either vacancy in the crystal structure or nongraphitic carbon) [21-22].

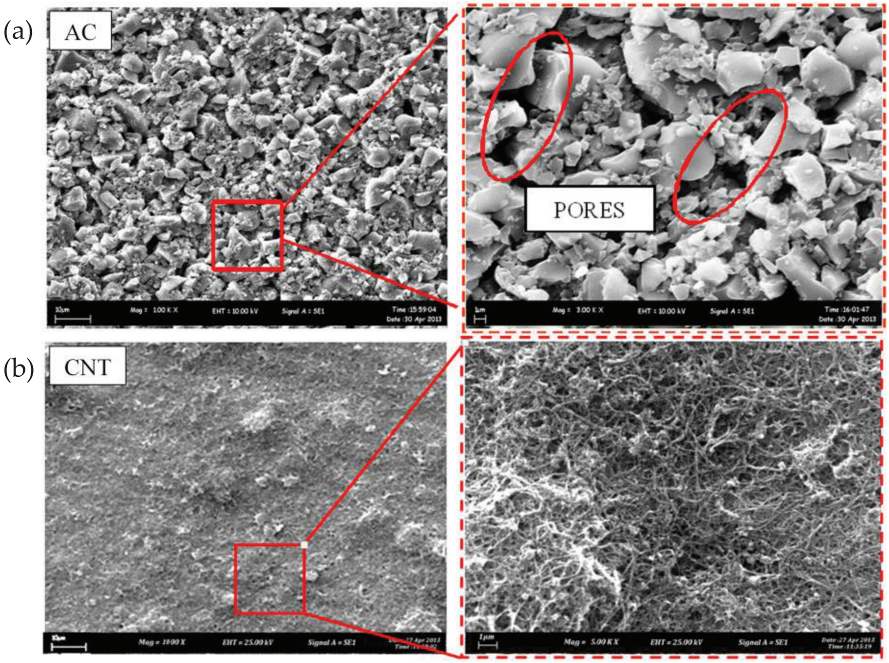

Figure 4: SEM surface images of (a) AC and (b) CNT coatings deposited by EPD at constant 80 V for a continuous 10 min

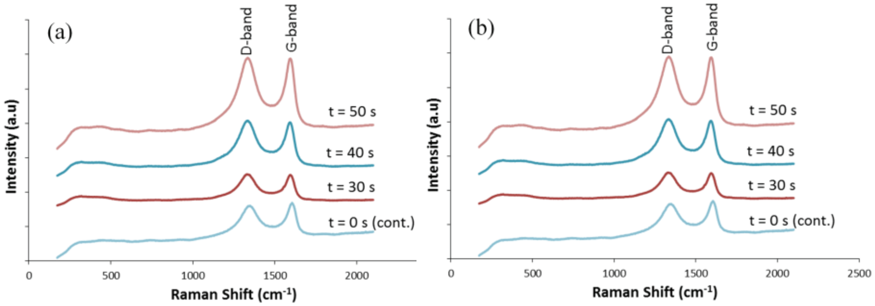

Figure 5: Raman spectra of: (a) AC and (b) CNT deposit formed by pulsed EPD at different pulse separation time and applied voltage of 80 V (t= 0 s refers to deposit formed by EPD at a continuous deposition time of 10 min)

I_G/I_D plot of the AC samples (Figure 6) remained constant at 1.0, although the deposit yield varied at different pulse separation times. It appeared that their graphitic carbon content ratios were not governed by the EDL compression mechanism (as suggested earlier). Generally, AC coating has lower graphitic carbon percentage than the CNT coating. Studies have shown that AC has an intrinsic nongraphitic crystal structures, consists of a high percentage of sp2-bonded atoms with the pentagonal structure [23]. This explains the uniform distribution of the defects throughout the AC particles, irrespective of the AC particle size or morphology.

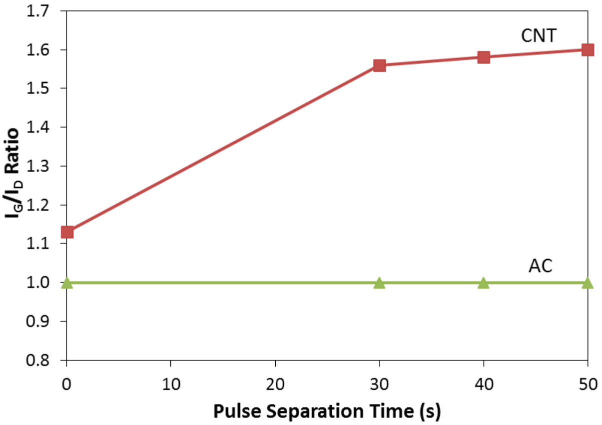

Figure 6: G-band /D-band peak intensity ratio of CNT and AC coatings deposited at different pulse separation time (applied voltage = 80 V)

Surprisingly, a large increment (38 %) in I_G/I_D ratio was observed when the continuous EPD mode was converted to the pulsed mode. A subsequent but gradual increment of the graphitic carbon content ratio at 4 % was observed when the pulse separation time increased from 30 to 50 s. The rise of the graphitic carbon content's decrease correlated directly with the CNT's yield decrease, suggesting the nongraphitic carbons were removed from the CNT coating, particularly at longer pulse separation times where a higher removal rate occurred. Since particle agglomerate disintegration from coating has been proposed to explain the CNT yield decrease, this could also suggest the nongraphitic carbon participated in the CNT particle agglomerate formation.

4.0 CONCLUSION

The present work compares the deposit yields and graphitic contents of carbon nanotube (CNT) and activated carbon (AC) electrode materials deposited by pulsed and continuous electrophoretic deposition (EPD) for electrochemical capacitor. For the pulsed EPD samples, AC yield displayed an incremental trend (Hamaker's rule) at the increasing voltage range (i.e. 30-80 V). However, the CNT's yield exhibited a decrease at a higher voltage. The decrease of the CNT's yield was due to the disintegration of the deposited CNT agglomerates from the CNT coating during the pulse EPD. The CNT agglomerates were formed prior to the EPD by the small nongraphitic carboneous particles. The removal of nongraphitic CNT agglomerates simultaneously raised the graphitic-nongraphitic content ratio in the deposited CNT coating. Furthermore, a higher graphitic carbon content was achieved at a longer pulse separation time in the CNT coating. The nongraphitic structure is an intrinsic feature of the AC particles, thus the agglomeration of AC particles during pulsed EPD did not significantly reduce the nongraphitic content in the AC coating. A future work is required to improve the suspension formulation for the EPD and process of CNT in order to minimize the deteriorating agglomeration effect on the CNT deposit yield.

ACKNOWLEDGEMENT

We acknowledge Ministry of Higher Education Malaysia and Universiti Teknikal Malaysia Melaka for the financial support (Grant No.: PJP/S01160).

REFERENCES

[1] D. Sheberla, J.C. Bachman, J.S. Elias, C.-J. Sun, S.-H. Yang and M. Dinca, "Conductive MOF electrodes for stable supercapacitors with high areal capacitance", *Nature Materials*, vol. 16, no. 2, pp. 220-224, 2017.

[2] R. Diaz-Delgado and A.P. Doherty, "Carbons, ionic liquids and quinones for electrochemical capacitors", *Frontiers in Materials*, vol. 3, pp. 1-7, 2016.

[3] E. Talib, K.T. Lau, M. Zaimi, M.S.A. Bistamam, N.S. Abdul Manaf, R.N.A. Raja Seman, N.N. Zulkapli and M.A. Azam, "Electrochemical performance of multi walled carbon nanotube and graphene composite films using electrophoretic deposition technique", *Applied Mechanics and Materials*, vol. 761, pp. 468-472, 2015.

[4] W. Gu and G. Yushin, "Review of nanostructured carbon materials for electrochemical capacitor applications: advantages and limitations of activated carbon, carbide ‐ derived carbon, zeolite ‐ templated carbon, carbon aerogels, carbon nanotubes, onion ‐ like carbon and graphene", *Wiley Interdisciplinary Reviews: Energy and Environment*, vol. 3, no. 5, pp. 424-473, 2014.

[5] Q. Wu, Y. Xu, Z. Yao, A. Liu and G. Shi, "Supercapacitors based on flexible graphene/polyaniline nanofiber composite films", *ACS Nano*, vol. 4, no. 4, pp. 1963-1970, 2010.

[6] A. Chávez-Valdez and A.R. Boccaccini, "Innovations in electrophoretic deposition: Alternating current and pulsed direct current methods", *Electrochimica Acta*, vol. 65, pp. 70-89, 2012.

[7] K.-T. Lau, M.H.R.A. Razak, S.-L. Kok, M. Zaimi, M.W.A. Rashid, N. Mohamad and M.A. Azam, "Electrophoretic Deposition and Heat Treatment of Steel-Supported PVDF-Graphite Composite Film", *Applied Mechanics and Materials*, vol. 761, pp. 412-416, 2015.

[8] S. Roy, R. Bajpai, N. Soin, S.S. Roy, J.A. McLaughlin and D.S. Misra, "Diameter control of single wall carbon nanotubes synthesized using chemical vapor deposition", *Applied Surface Science*, vol. 321, pp. 70-79, 2014.

[9] N.S.A. Manaf, M.S.A. Bistamam and M.A. Azam, "Development of high performance electrochemical capacitor: A systematic review of electrode fabrication technique based on different carbon materials", *ECS Journal of Solid State Science and Technology*, vol. 2, no. 10, pp. M3101-M3119, 2013.

[10] N. Arora and N.N. Sharma, "Arc discharge synthesis of carbon nanotubes: Comprehensive review", *Diamond and Related Materials*, vol. 50, pp. 135-150, 2014.

[11] M. Ammam, "Electrophoretic deposition under modulated electric fields: A review", *RSC Advances*, vol. 2, no. 20, pp. 7633-7646, 2012.

[12] B. Neirinck, O. Van Der Biest and J. Vleugels, "A current opinion on electrophoretic deposition in pulsed and alternating fields", *The Journal of Physical Chemistry B*, vol. 117, no. 6, pp. 1516-1526, 2013.

[13] S.-C. Wang and B.-C. Huang, "Field emission properties of Ag/SiO2/carbon nanotube films by pulsed voltage co-electrophoretic deposition", *Thin Solid Films*, vol. 517, no. 3, pp. 1245-1250, 2008.

[14] A. Benko, A. Przekora, A. Wesełucha-Birczyńska, M. Nocuń, G. Ginalska and M. Błażewicz, "Fabrication of multi-walled carbon nanotube layers with selected properties via electrophoretic deposition: physicochemical and biological characterization", *Applied Physics A*, vol. 122, no. 4, pp. 1-13, 2016.

[15] J. Lim, M. Jalali and S.A. Campbell, "Electrophoretic deposition of single wall carbon nanotube films and characterization", *MRS Proceedings*, vol. 1752, pp. 59-63, 2015.

[16] H. Wang, "Dispersing carbon nanotubes using surfactants", *Current Opinion in Colloid & Interface Science*, vol. 14, no. 5, pp. 364-371, 2009.

[17] H.C. Hamaker, "Formation of a deposit by electrophoresis", *Transactions of the Faraday Society*, vol. 36, pp. 279-287, 1940.

[18] K.-T. Lau and C.C. Sorrell, "Effect of charging agents on electrophoretic deposition of titanium particles", *Journal of the Australian Ceramic Society*, vol. 49, no. 2, pp. 104-112, 2013.

[19] P.J. Harris, Z. Liu and K. Suenaga, "Imaging the atomic structure of activated carbon", *Journal of Physics: Condensed Matter*, vol. 20, no. 36, p. 362201, 2008.

[20] W.F. Smith and J. Hashemi, *Foundations of Materials Science and Engineering, 4th Edition*. New York: McGraw Hill, 2006.

[21] E. Steven, W.R. Saleh, V. Lebedev, S.F. Acquah, V. Laukhin, R.G. Alamo and J.S. Brooks, "Carbon nanotubes on a spider silk scaffold", *Nature Communications*, vol. 4, pp. 1-8, 2013.

[22] S. Osswald, E. Flahaut, H. Ye and Y. Gogotsi, "Elimination of D-band in Raman spectra of double-wall carbon nanotubes by oxidation", *Chemical Physics Letters*, vol. 402, no. 4-6, pp. 422-427, 2005.

[23] J.-S. Roh, "Structural Study of the Activated Carbon Fiber using Laser Raman Spectroscopy", *Carbon Letters*, vol. 9, no. 2, pp. 127-130, 2008.